Journal of Computational Mathematics
Vol.xx, No.x, 2024, 1–24.
http://www.global-sci.org/jcm
doi:10.4208/jcm.2210-m2022-0085

# RECONSTRUCTION-BASED A POSTERIORI ERROR ESTIMATES FOR THE L1 METHOD FOR TIME FRACTIONAL PARABOLIC PROBLEMS*

Jiliang Cao
*Department of Mathematics, Shanghai Normal University, Shanghai 200234, China*
*Hunan Key Laboratory for Computation and Simulation in Science and Engineering & Key Laboratory of Intelligent Computing and Information Processing of Ministry of Education, Xiangtan University, Xiangtan 411105, China*
Aiguo Xiao
*Hunan Key Laboratory for Computation and Simulation in Science and Engineering & Key Laboratory of Intelligent Computing and Information Processing of Ministry of Education, Xiangtan University, Xiangtan 411105, China*
*Email: xag@xtu.edu.cn*
Wansheng Wang[1)]
*Department of Mathematics, Shanghai Normal University, Shanghai 200234, China*
*Email: w.s.wang@163.com*

**Abstract**

In this paper, we study a posteriori error estimates of the L1 scheme for time discretizations of time fractional parabolic differential equations, whose solutions have generally the initial singularity. To derive optimal order a posteriori error estimates, the quadratic reconstruction for the L1 method and the necessary fractional integral reconstruction for the first-step integration are introduced. By using these continuous, piecewise time reconstructions, the upper and lower error bounds depending only on the discretization parameters and the data of the problems are derived. Various numerical experiments for the one-dimensional linear fractional parabolic equations with smooth or nonsmooth exact solution are used to verify and complement our theoretical results, with the convergence of $\alpha$ order for the nonsmooth case on a uniform mesh. To recover the optimal convergence order $2-\alpha$ on a nonuniform mesh, we further develop a time adaptive algorithm by means of barrier function recently introduced. The numerical implementations are performed on nonsmooth case again and verify that the true error and a posteriori error can achieve the optimal convergence order in adaptive mesh.

*Mathematics subject classification:* 65M15, 65M50, 65M06, 65M12, 35R11, 26A33.
*Key words:* Time fractional parabolic differential equations, A posteriori error estimates, L1 method, Fractional integral reconstruction, Quadratic reconstruction.

## 1. Introduction

Adaptive methods have become very popular and powerful tools for certain classes of PDEs. A posteriori error analysis can provide information about the error introduced by discretization and is at the base of adaptive computation. Time adaptive algorithms are naturally related to error control and variable time step-sizes. In this paper we derive a posteriori error estimates

* Received April 10, 2022 / Revised version received October 10, 2022 / Accepted October 24, 2022 / Published online January 23, 2024 /
1) Corresponding author

for time discretization by the L1 method for abstract time fractional parabolic differential equations (TFPDEs) and construct an adaptive algorithm based on this rigorous a posteriori error estimates. To do this, we first introduce functional space and corresponding norms.

### 1.1. Functional space and norms

Let $H$ be a Hilbert space with inner product $(\cdot\,,\cdot)$. We identify $H$ with its dual. Let $A$: $D(A) \to H$ be a positive definite, self-adjoint, linear operator on $H$ with domain $D(A)$ being dense in $H$. Let $V := D(A^{1/2})$ and denote the norms in $H$ and $V$ by $\|\cdot\|$ and $\|\cdot\|_1, \|v\|_1 = \|A^{1/2}v\| = (Av, v)^{1/2}$, respectively. Let $V^*$ be the dual of $V$, and denote by $\|\cdot\|_{-1}$ the dual norm on $V^*, \|v\|_{-1} = \|A^{-1/2}v\| = (v, A^{-1}v)^{1/2}$. We still denote by $(\cdot\,,\cdot)$ the duality pairing between $V^*$ and $V$. In a natural way the Lebesgue spaces $L^p(J;X)$ with a time interval $J = [t_*, t^*]$ and Banach space $X$ (here, $X = H, V$ or $V^*$), $1 \le p < \infty$, consist of all those functions $u(t)$ that take values in $X$ for almost every $t \in J$ such that the $L^p$ norm of $\|u(t)\|_X$, i.e.

$$\|u\|_{L^p(J;X)} = \left(\int_J \|u(t)\|_X^p dt\right)^{\frac{1}{p}}$$

is finite. For $p = \infty, L^\infty(J;X)$ is the space of (classes of) measurable functions from $J$ into $X$ which are essentially bounded, the space is Banach for the norm

$$\|u\|_{L^\infty(J;X)} := \operatorname*{ess\,sup}_{t\in J} \|u(t)\|_X.$$

Note that for continuous function $u(t)$, we have $\|u\|_{L^\infty(J;X)} = \max_{t\in J} \|u(t)\|_X$. For simplicity, we will write $L^p(0,t;X)$ for $L^p((0,t);X)$.

Let $\partial_t^\alpha$ denote the Caputo fractional derivative of order $\alpha$ $(0 < \alpha < 1)$ with respect to $t$ defined by

$$\partial_t^\alpha u(t) := \int_0^t \omega_{1-\alpha}(t-s)u'(s)ds, \quad \omega_\alpha(t) = \frac{t^{\alpha-1}}{\Gamma(\alpha)},$$

where $\Gamma(z)$ is the Gamma function,

$$\Gamma(z) := \int_0^\infty s^{z-1}e^{-s}ds, \quad \Re(z) > 0.$$

We define the Riemann-Liouville fractional integral operator of order $\beta$ $(\beta \ge 0)$ as

$$I_t^\beta u(t) = \int_0^t \omega_\beta(t-s)u(s)ds, \quad t > 0$$

with $I_t^0 u(t) = u(t)$ [44]. Then we recall the relationship between the Riemann-Liouville fractional derivative and Caputo fractional derivative

$$\partial_t^\alpha u(t) = \frac{d}{dt}\left\{I_t^{1-\alpha}[u(t)-u(0)]\right\} = \frac{d}{dt}\left\{\int_0^t \omega_{1-\alpha}(t-s)[u(s)-u(0)]ds\right\},$$

and the relationship of the Riemann-Liouville fractional integral and Riemann-Liouville fractional derivative [54]:

$$\partial_t^{-\alpha} u(t) = I_t^\alpha u(t) = \int_0^t \omega_\alpha(t-s)u(s)ds, \quad t > 0. \tag{1.1}$$

To avoid too clumsy a notation, we will introduce the space

$$L^p_\alpha(0,t;X) := \left\{ u \,\middle|\, (I^\alpha_t \|u(t)\|^p_X)^{\frac{1}{p}} < \infty \right\}$$

with the norm

$$\|u\|_{L^p_\alpha(0,t;X)} = \left(I^\alpha_t \|u(t)\|^p_X\right)^{\frac{1}{p}}.$$

In the following analysis, we will use frequently the inequality

$$\omega_\alpha(t)\|u\|^p_{L^p(0,t;X)} \le \|u\|^p_{L^p_\alpha(0,t;X)}, \tag{1.2}$$

which can be found in [24].

### 1.2. Numerical methods for TFPDEs

Consider abstract TFPDEs

$$\begin{cases} \partial^\alpha_t u(t) + Au(t) = f(t), \quad t \in (0,T], \\ u(0) = u_0, \end{cases} \tag{1.3}$$

where $T > 0$ is a fixed final time, $u_0 \in H$ is a given initial data, and the forcing term $f$ is a sufficiently smooth function.

Since the class of time-dependent problems (1.3) arise in various models of physical processes (see [20, 31, 42] and references therein), these problems and their numerical approximations have attracted much attention in recent years; see, e.g. recent literature [3, 8, 10, 20, 23, 49, 61]. There are several predominant classes of numerical methods for discretizing the time fractional derivative. Here we mention the convolution quadrature (CQ) [3, 7, 9, 12, 18, 21–23, 38–40, 49, 58–60], the spectral methods [13, 18, 20, 23, 30, 31, 36, 45], and the finite difference type methods, etc.

CQ inherits excellent numerical stability property of the underlying schemes for ODEs, but it is often restricted to uniform mesh. And spectral methods show high order of accuracy for TFPDEs with smooth solutions, but the solution $u$ usually has a weak singularity near $t = 0$, even for a very smooth source term $f$ (see, e.g. [13, 17, 18, 20, 23, 43, 45]). The finite difference type schemes are based on piecewise polynomial approximation, especially interpolation, and the most prominent one is the L1 scheme. Since its first appearance, the L1 scheme and its variant have been extensively used in practice and currently it is one of the most popular and basic numerical methods for solving the time fractional diffusion equations (see, e.g. [6, 8, 10–12, 14–16, 19, 28, 29, 32–35, 41, 45, 46, 55, 56]), because it is very flexible in construction and implementation and can generalize easily to nonuniform mesh. Thus, in this paper, we will focus on this scheme.

For the L1 scheme, the stability and a priori error estimates have been the subject of much research in recent years. It was shown in [35,46] that the local truncation error of the L1 approximation is bounded by $ck^{2-\alpha}$, where the constant $c$ depends on $\|u\|_{C^2([0,T])}$ and $k$ is the maximum time step-size. Therefore, it requires that the solution $u$ be twice continuously differentiable in time, which is usually unsatisfying for problems with initial singularity. In fact, an $\mathcal{O}(k)$ convergence rate for both smooth and nonsmooth initial data was established in [19]. Recently, to recover the optimal convergence order $\mathcal{O}(k^{2-\alpha})$ for nonsmooth solutions in $L^\infty(0,T;H)$, some special nonuniform mesh have been proposed by taking into account the initial singularity in the problems (1.3), such as graded mesh, quasi-graded mesh, general nonuniform mesh, and so on (see, e.g. [25, 27, 33, 45, 55]). However, the graded mesh $t_n = T(n/N)^\gamma$ depends on the regularity of the exact solution and the general nonuniform mesh has the constraint

$$k_{n-1} \leq k_n, \tag{1.4}$$

where $k_n = t_n - t_{n-1}$ is the time step-size with $t_n$ being mesh points. This motives researchers to provide error estimates on nonuniform grids under minimal regularity of the solution or by removing the constraint of the time step-size.

### 1.3. A posteriori error estimates

A posteriori error estimates can be viewed as such type of error estimates which can be quantified for a given simulation, knowing only the problem data and approximate solution. Such computable a posteriori error estimates have been investigated by many researchers for various numerical methods for integer-order parabolic problems during the last decades (see, e.g. [1, 5, 37, 47, 50–53]). A posteriori error estimates and adaptivity are now in many cases very successful tools for efficient numerical computations of linear as well as nonlinear integer-order problems. For TFPDEs (1.3), however, to the best of our knowledge, there is few article in the literature concerning a posteriori error analysis of numerical methods for time fractional differential equations and their adaptive algorithms except very limited works on the Galerkin spectral method [57, 62] and the space-time spectral method [48]. It is worth noting that the pointwise-in-time a posteriori error control for TFPDEs was proposed in [26] by using the barrier function, and a posteriori error estimates of the L1 method or CQ for TFPDEs are derived in [4]. Different form a posteriori error estimates based on the linear reconstruction in [4, 26], we devoted to deriving a posteriori error estimates based on quadratic reconstruction, which is shown to perform better on both smooth and nonsmooth problems from numerical experiments. The numerical results of Example 3.1 show that, even for the smooth solution problem, the residual of L1 method based on the linear reconstruction converges only of the first order, which does not match the optimal order of the L1 method. Therefore it is necessary to provide optimal a posteriori error estimates by means of the quadratic reconstruction. The main difficulty in deriving the optimal order a posteriori error estimates for the finite difference type methods is to obtain the error equations which involves long-range history dependence. In this paper, we will address this issue. The main contribution of this paper is to derive a posteriori error estimates which solely depend on the discrete solution and data, and construct adaptive algorithms based on rigorous a posteriori error control. We point out that in our a posteriori error estimates, no extra regularity of the solution $u$ has been used, as well as no constraints such as (1.4) between consecutive time-steps. As a consequence, the a posteriori error control provides a practical, as well as mathematically sound, means for detecting singularity phenomena and doing reliable computations with flexible time step-size $k_n$.

### 1.4. Outline

We start Section 2 by introducing necessary assumptions and notation as well as the L1 method for the problems (1.3). For a continuous approximation $U$ in time, a posteriori error bounds based on linear reconstruction are derived for the fractional order equations by using the energy techniques, but they are not the optimal convergence order $\mathcal{O}(k^{2-\alpha})$ . To obtain the optimal convergence order $\mathcal{O}(k^{2-\alpha})$ for the a posteriori error estimates, the natural quadratic reconstruction $\widehat{U}$ is introduced in Section 4. In this section the fractional integral reconstruction for the first-step integration is also introduced. Different from the numerical methods for the integer-order parabolic equations, it seems impossible to derive a posteriori error estimates for this type of reconstructions which are based on differential equations when the number of the L1 integration step is large. Furthermore, a posteriori error estimates in the $L^2_\alpha(0,t;V)$-, $L^2(0,t;V)$- and $L^\infty(0,t;H)$-norms are derived for the L1 method in Section 5. A numerical study is carried out for several test cases with smooth or nonsmooth solutions in Section 6. We further develop a time adaptive algorithm in Section 7. The last section, Section 8, will contain a few concluding remarks.

## 2. L1 Method for TFPDEs

Now we consider the L1 method for solving TFPDEs (1.3). Let $0 = t_0 < t_1 < \cdots < t_N = T$ be a partition of $[0,T]$, $I_n := [t_{n-1}, t_n]$, and $k_n := t_n - t_{n-1}$, which in general will be variable. The Caputo fractional derivative $\partial_t^\alpha u$, which can be written as

$$\partial_t^\alpha u(t_n) = \frac{1}{\Gamma(1-\alpha)} \sum_{j=1}^{n} \int_{t_{j-1}}^{t_j} (t_n - s)^{-\alpha} u'(s) ds,$$

is approximated by the classical L1 approximation

$$\begin{aligned}\bar\partial_t^\alpha U^n &= \sum_{j=1}^{n} \frac{U^j - U^{j-1}}{k_j} \int_{t_{j-1}}^{t_j} \omega_{1-\alpha}(t_n - s) ds \\ &= \frac{1}{\Gamma(2-\alpha)} \sum_{j=1}^{n} \frac{U^j - U^{j-1}}{k_j} \left[(t_n - t_{j-1})^{1-\alpha} - (t_n - t_j)^{1-\alpha}\right] \\ &= \sum_{j=1}^{n} a_j(t_n) \bar\partial U^j, \end{aligned} \tag{2.1}$$

where

$$\bar\partial U^j := \frac{U^j - U^{j-1}}{k_j}, \quad a_j(t) := \frac{1}{\Gamma(2-\alpha)} \left[(t - t_{j-1})^{1-\alpha} - (t - t_j)^{1-\alpha}\right].$$

It can be observed from (2.1) that it approximates the function $u$ by a continuous piecewise linear interpolation, similar to the backward Euler method. The L1 method for TFPDEs (1.3) is then defined as follows:

$$\bar\partial_t^\alpha U^n + AU^n = f^n, \quad n \ge 1, \tag{2.2}$$

where $f^n := f(t_n)$. The continuous piecewise linear approximation to $u$ or the linear reconstruction of $U^n$ can be expressed in terms of its nodal values,

$$\begin{aligned} U(t) &= \frac{t_n - t}{k_n} U^{n-1} + \frac{t - t_{n-1}}{k_n} U^n \\ &= \ell_{n,-1}(t) U^{n-1} + \ell_{n,1}(t) U^n \\ &= U^{n-1} + (t - t_{n-1}) \bar\partial U^n, \quad t \in I_n, \end{aligned} \tag{2.3}$$

where

$$\ell_{n,-1}(t) = \frac{t_n - t}{k_n}, \quad \ell_{n,1}(t) = \frac{t - t_{n-1}}{k_n}.$$

From (2.3) we get

$$AU(t) = AU^{n-1} + A(t - t_{n-1}) \bar\partial U^n, \quad t \in I_n.$$

In view of (2.2) and (2.3), we also have

$$\begin{aligned}AU(t) &= \frac{t_n - t}{k_n} AU^{n-1} + \frac{t - t_{n-1}}{k_n} AU^n \\ &= \frac{t_n - t}{k_n}\left(f^{n-1} - \bar{\partial}_t^\alpha U^{n-1}\right) + \frac{t - t_{n-1}}{k_n}\left(f^n - \bar{\partial}_t^\alpha U^n\right) \\ &= \tilde{f}(t) - \left(\frac{t_n - t}{k_n}\bar{\partial}_t^\alpha U^{n-1} + \frac{t - t_{n-1}}{k_n}\bar{\partial}_t^\alpha U^n\right), \quad t \in I_n, \end{aligned} \tag{2.4}$$

where $\tilde{f}(t)$ denotes the linear approximation of $f(t)$

$$\tilde{f}(t) = \ell_{n,-1}(t) f^{n-1} + \ell_{n,1}(t) f^n, \quad t \in I_n. \tag{2.5}$$

Since $U$ is a linear function on $I_n$, we have $U'(t) = \bar{\partial} U^n$. Then for $t \in I_n$, one gets

$$\begin{aligned}\partial_t^\alpha U(t) &= \int_0^t \omega_{1-\alpha}(t-s) U'(s) ds \\ &= \frac{1}{\Gamma(1-\alpha)} \sum_{j=1}^{n-1} \int_{t_{j-1}}^{t_j} (t-s)^{-\alpha} U'(s) ds + \frac{1}{\Gamma(1-\alpha)} \int_{t_{n-1}}^{t} (t-s)^{-\alpha} U'(s) ds \\ &= \sum_{j=1}^{n-1} a_j(t) \bar{\partial} U^j + \frac{(t - t_{n-1})^{1-\alpha}}{\Gamma(2-\alpha)} \bar{\partial} U^n. \end{aligned} \tag{2.6}$$

## 3. A Posteriori Error Estimates of the Linear Reconstruction

Assume that a continuous approximation $U(t)$ to $u(t)$, for all $t \in [0, T]$, has been obtained by a numerical method such as the L1 method with interpolation. We define the residual of $U$ as

$$R(t) = \partial_t^\alpha U(t) + AU(t) - f(t) \in H, \quad t \in I_n. \tag{3.1}$$

Then the error $E := u - U$ satisfies the equation

$$\partial_t^\alpha E(t) + AE(t) = -R(t). \tag{3.2}$$

Hence, we have the following a posteriori error estimate of the linear reconstruction.

**Theorem 3.1 ($L^2(0,T;V)$ and $L^2_\alpha(0,T;V)$ Error Estimates).** *Let $U(t)$ be the L1 approximation to the solution of problems (1.3), and the error $E(t) := u(t) - U(t)$. Then the following a posteriori error estimate is valid, for $t \in I_n$, $n \geq 1$,*

$$\begin{aligned}\|E(t)\|^2 + \omega_\alpha(t) \|E\|^2_{L^2(0,t;V)} &\leq \|E(t)\|^2 + \|E\|^2_{L^2_\alpha(0,t;V)} \\ &\leq \|E(0)\|^2 + \|R\|^2_{L^2_\alpha(0,t;V^*)}. \end{aligned} \tag{3.3}$$

*Proof.* Taking in (3.2) the inner product with $E(t)$, we obtain, for any $t \in I_n$, $n \geq 1$,

$$\left(\partial_t^\alpha E(t), E(t)\right) + \|E(t)\|_1^2 \leq -\left(R(t), E(t)\right).$$

Using the Cauchy-Schwarz inequality, we get

$$\left(\partial_t^\alpha E(t), E(t)\right) + \|E(t)\|_1^2 \leq \|R(t)\|_{-1} \|E(t)\|_1 \leq \frac{1}{2}\left(\|R(t)\|_{-1}^2 + \|E(t)\|_1^2\right). \tag{3.4}$$

Applying the result (see, for example, [2])

$$\big(\partial_t^\alpha E(t), E(t)\big) \geq \frac{1}{2}\partial_t^\alpha \|E(t)\|^2,$$

to (3.4), we obtain

$$\partial_t^\alpha \|E(t)\|^2 + \|E(t)\|_1^2 \leq \|R(t)\|_{-1}^2. \tag{3.5}$$

Now use the Riemann-Liouville fractional integral operator $I_t^\alpha$ on both sides of (3.5). An application of the relation (1.1) yields

$$\|E(t)\|^2 + \|E\|^2_{L^2_\alpha(0,t;V)} \leq \|E(0)\|^2 + \|R\|^2_{L^2_\alpha(0,t;V^*)}.$$

Using inequality (1.2), we obtain the required results and thus complete the proof. □

Now we want to estimate the residual $R(t)$, which has been introduced in (3.1). For the L1 scheme (2.2), the residual can be written as

$$R(t) = \partial_t^\alpha U(t) - \bar{\partial}_t^\alpha U^n + A[U(t) - U^n] - [f(t) - f^n], \quad t \in I_n,$$

where, in view of (2.1) and (2.6),

$$\partial_t^\alpha U(t) - \bar{\partial}_t^\alpha U^n = \sum_{j=1}^{n-1} \bar{\partial} U^j \left[a_j(t) - a_j(t_n)\right] + \frac{(t - t_{n-1})^{1-\alpha} - k_n^{1-\alpha}}{\Gamma(2-\alpha)} \bar{\partial} U^n.$$

In the following numerical example, we will observe that $R(t)$ is an a posteriori quantity of first order with respect to the time step-size $k_n$. Therefore, applying (3.3) leads inevitably to suboptimal bounds, since the L1 method (2.2) is of $(2-\alpha)$-order accuracy for sufficiently regular problem.

**Example 3.1.** Let us consider the following model problem on $\Omega = (0,1)$:

$$\begin{cases} \partial_t^\alpha u = \dfrac{\partial^2 u}{\partial x^2} + f, & x \in \Omega, \quad 0 \leq t \leq 1, \\ u(0,t) = u(1,t) = 0, & 0 \leq t \leq 1, \\ u(x,0) = u_0(x) = x(1-x). \end{cases} \tag{3.6}$$

We prescribe the exact solution of the problem as $u(x,t) = (1+t^2)x(1-x)$. Then the corresponding source function is

$$f(x,t) = \frac{\Gamma(3)}{\Gamma(3-\alpha)} t^{2-\alpha} x(1-x) + 2(1+t^2).$$

The space derivative $\partial^2/\partial x^2$ of (3.6) will be approximated with central finite difference of second order. After spatial discretization a system of fractional ordinary differential equations results,

$$\begin{aligned} &\partial_t^\alpha v_i(t) = \Delta x^{-2}[v_{i-1}(t) - 2v_i(t) + v_{i+1}(t)] + f_i(t), && 0 \leq t \leq 1, \\ &v_0(t) = v_M(t) = 0, && 0 \leq t \leq 1, \\ &v_i(0) = x_i(1-x_i), && i = 1, 2, \ldots, M-1, \end{aligned}$$

where $M = 1/\Delta x, x_i = i\Delta x, v_i(t)$ is meant to approximate the solution of (3.6) at the point $(t, x_i)$, and $f_i$ stands for $f$ at $(t, x_i)$. We use a uniform time partition for $[0,T]$, that is $k = 1/N$.

The errors $\|E(T)\|$, $\|E\|_{L^2_\alpha(0,T;V)}$, the residual $\|R\|_{L^2_\alpha(0,T;V^*)}$ and their convergence orders are presented in Table 3.1. It should be mentioned that the dual norm $\|v\|_{-1}$ is computed by using the definition $\|v\|_1 = \|A^{1/2}v\| = (Av,v)^{1/2}$, where $A$ is the finite difference discrete matrix. As for the norm $\|u\|_{L^p_\alpha(0,t;X)}$, we approximate the fractional integral by the Gauss-Legendre quadrature formula with weight functions and three nodes. But it is worth mentioning, from the definition of the norm $\|u\|_{L^p_\alpha(0,t;X)}$, that the integration does not make sense when the variable $s$ is close to $t$ due to the singular kernel $\omega_\alpha(t-s)$, so we have to regard the singular kernel as the weight functions at the last subintervals.

From Table 3.1, we observe that the error $\|E\|_{L^2_\alpha(0,T;V)}$ is of order $2-\alpha$, but the residual $\|R\|_{L^2_\alpha(0,T;V^*)}$ is only of order 1, even for sufficiently regular problem. This motives us to provide optimal a posteriori error estimators.

Table 3.1: The errors $\|E(T)\|$, $\|E\|_{L^2_\alpha(0,T;V)}$, the residual $\|R\|_{L^2_\alpha(0,T;V^*)}$ and their convergence orders in time, where $T=1$ and $M=512$.

| $\alpha$ | $N$ | $\|E(T)\|$ | Order | $\|E\|_{L^2_\alpha(0,T;V)}$ | Order | $\|R\|_{L^2_\alpha(0,T;V^*)}$ | Order |
|---|---|---|---|---|---|---|---|
| 0.25 | 16 | 2.9585E-05 | - | 4.4990E-04 | - | 5.8592E-02 | - |
| | 32 | 9.2304E-06 | 1.6804 | 1.2075E-04 | 1.8975 | 3.1311E-03 | 0.9040 |
| | 64 | 2.8527E-06 | 1.6940 | 3.2420E-05 | 1.8970 | 1.6484E-03 | 0.9255 |
| | 128 | 8.7525E-07 | 1.7045 | 8.7236E-06 | 1.8939 | 8.5840E-04 | 0.9414 |
| 0.5 | 16 | 1.2098E-04 | - | 7.7997E-04 | - | 6.4303E-02 | - |
| | 32 | 4.3485E-05 | 1.4762 | 2.3840E-04 | 1.7100 | 3.3323E-02 | 0.9483 |
| | 64 | 1.5551E-05 | 1.4835 | 7.4817E-05 | 1.6719 | 1.7089E-02 | 0.9634 |
| | 128 | 5.5421E-06 | 1.4884 | 2.4070E-05 | 1.6361 | 8.6996E-03 | 0.9740 |
| 0.75 | 16 | 3.9180E-04 | - | 1.5779E-03 | - | 6.0377E-02 | - |
| | 32 | 1.6542E-04 | 1.2439 | 6.0398E-04 | 1.3854 | 3.0684E-02 | 0.9765 |
| | 64 | 6.9720E-05 | 1.2465 | 2.3904E-04 | 1.3372 | 1.5512E-02 | 0.9840 |
| | 128 | 2.9355E-05 | 1.2479 | 9.6772E-05 | 1.3045 | 7.8150E-03 | 0.9890 |

## 4. Quadratic Reconstructions for Numerical Solution

To obtain optimal order a posteriori error estimate for the L1 method, we shall introduce numerical reconstruction solution $\widehat{U}$.

### 4.1. Fractional integral reconstruction for the first-step integration

For $t \in I_1$, we introduce the fractional integral reconstruction. We define the reconstruction as, for $t \in I_1$,

$$\begin{aligned}
\widehat{U}(t) &= U^0 - \partial_t^{-\alpha} AU(t) + \partial_t^{-\alpha} P_1 f(t) \\
&= U^0 - \int_0^t \omega_\alpha(t-s) AU(s)ds + \int_0^t \omega_\alpha(t-s) P_1 f(s) ds \\
&= U^0 - \frac{1}{\Gamma(\alpha+2)} t^{\alpha+1} A\bar{\partial} U^1 - \frac{1}{\Gamma(\alpha+1)} t^\alpha AU^0 + \int_0^t \omega_\alpha(t-s) P_1 f(s) ds \\
&= U(t) - t\bar{\partial} U^1 - \frac{1}{\Gamma(\alpha+2)} t^{\alpha+1} A\bar{\partial} U^1 - \frac{1}{\Gamma(\alpha+1)} t^\alpha AU^0
\end{aligned}$$

$$+\int_0^t \omega_\alpha(t-s)P_1 f(s)ds, \tag{4.1}$$

where $P_1$ denotes the $L^2$ orthogonal projection operator or the linear interpolation operator onto the space of linear polynomials in $I_1$. From (4.1), it is easy to obtain the following pointwise equation:

$$\partial_t^\alpha \widehat{U}(t) + AU(t) = P_1 f(t), \quad \forall\, t \in I_1. \tag{4.2}$$

Then the residual $\widehat{R}(t)$ can be defined as

$$\widehat{R}(t) = \partial_t^\alpha \widehat{U}(t) + A\widehat{U}(t) - f(t), \tag{4.3}$$

and further written in the form

$$\widehat{R}(t) = A[\widehat{U}(t) - U(t)] + [P_1 f(t) - f(t)].$$

Therefore, it is easy to verify that the residual $\widehat{R}(t)$ defined in (4.3) is of order 2 when $t \in I_1$ and $f$ is sufficient smooth. From (1.3) and (4.2), we know that for $t \in I_1$, it holds that

$$\partial_t^\alpha \widehat{E}(t) + AE(t) = R_1(t), \tag{4.4}$$

where $\widehat{E}(t) = u(t) - \widehat{U}(t)$ and $R_1(t) = f(t) - P_1 f(t)$.

### 4.2. Quadratic reconstruction

For deriving a posteriori error bounds with $(2-\alpha)$-order accuracy for the L1 method (2.2), we shall introduce quadratic reconstruction, which is natural for the L1 method for TFPDEs (1.3), i.e.

$$\begin{aligned}\widehat{U}(t) &:= U(t) + \frac{1}{2}(t-t_{n-1})(t-t_n)\widehat{W}^n \\ &= U^{n-1} + (t-t_{n-1})\bar{\partial}U^n + \frac{1}{2}(t-t_{n-1})(t-t_n)\widehat{W}^n, \quad t \in I_n\end{aligned} \tag{4.5}$$

for $n \geq 2$, where

$$\widehat{W}^n = \frac{2(\bar{\partial}U^n - \bar{\partial}U^{n-1})}{k_n + k_{n-1}}.$$

Then by the definition of the Caputo fractional derivative, we have

$$\begin{aligned}\partial_t^\alpha \widehat{U}(t) &= \int_0^t \omega_{1-\alpha}(t-s)\widehat{U}'(s)ds \\ &= \partial_t^\alpha U(t) + \sum_{j=2}^{n-1} \widehat{W}^j \int_{t_{j-1}}^{t_j} \omega_{1-\alpha}(t-s)\big(s - t_{j-\frac{1}{2}}\big)ds \\ &\quad + \widehat{W}^n \int_{t_{n-1}}^{t} \omega_{1-\alpha}(t-s)\big(s - t_{n-\frac{1}{2}}\big)ds \\ &\quad + \int_0^{t_1} \omega_{1-\alpha}(t-s)\left[\frac{s^\alpha}{\Gamma(\alpha+1)}(\bar{\partial}f^1 - A\bar{\partial}U^1) + \frac{s^{\alpha-1}}{\Gamma(\alpha)}(f^0 - AU^0)\right]ds \\ &\quad - \frac{\bar{\partial}U^1}{\Gamma(2-\alpha)}\left[t^{1-\alpha} - (t-t_1)^{1-\alpha}\right].\end{aligned}$$

Using integration by parts, we further obtain

$$\partial_t^\alpha \widehat{U}(t) = \partial_t^\alpha U(t) + \mathcal{W}^n, \tag{4.6}$$

where $\mathcal{W}^n$ is defined by

$$\begin{aligned}
\mathcal{W}^n = &-\frac{1}{2\Gamma(2-\alpha)} \sum_{j=2}^{n-1} \widehat{W}^j k_j \left[(t-t_j)^{1-\alpha} + (t-t_{j-1})^{1-\alpha}\right] \\
&- \frac{1}{\Gamma(3-\alpha)} \sum_{j=2}^{n-1} \widehat{W}^j \left[(t-t_j)^{2-\alpha} - (t-t_{j-1})^{2-\alpha}\right] \\
&- \frac{\widehat{W}^n k_n}{2\Gamma(2-\alpha)} (t-t_{n-1})^{1-\alpha} + \frac{\widehat{W}^n}{\Gamma(3-\alpha)} (t-t_{n-1})^{2-\alpha} \\
&+ \frac{1}{\Gamma(1-\alpha)} \int_0^{t_1} (t-s)^{-\alpha} \left[\frac{s^\alpha}{\Gamma(\alpha+1)} (\bar{\partial} f^1 - A\bar{\partial} U^1) + \frac{s^{\alpha-1}}{\Gamma(\alpha)} (f^0 - AU^0)\right] ds \\
&- \frac{\bar{\partial} U^1}{\Gamma(2-\alpha)} \left[t^{1-\alpha} - (t-t_1)^{1-\alpha}\right].
\end{aligned} \tag{4.7}$$

Let $\widehat{E} = u - \widehat{U}$. Then it follows from (1.3), (4.6) and (2.4) that

$$\partial_t^\alpha \widehat{E}(t) + AE(t) = R_n(t), \quad n \geq 2, \tag{4.8}$$

where $R_n(t)$ is defined by

$$\begin{aligned}
R_n(t) &= f - \tilde{f} + \left(\ell_{n,-1} \bar{\partial}_t^\alpha U^{n-1} + \ell_{n,1} \bar{\partial}_t^\alpha U^n\right) - \partial_t^\alpha U(t) - \mathcal{W}^n \\
&= f - \tilde{f} + \sum_{j=1}^{n-1} \left[\left(\ell_{n,-1} a_j(t_{n-1}) + \ell_{n,1} a_j(t_n)\right) - a_j(t)\right] \bar{\partial} U^j \\
&\quad + \frac{t-t_{n-1}}{\Gamma(2-\alpha)} \left(k_n^{-\alpha} - (t-t_{n-1})^{-\alpha}\right) \bar{\partial} U^n - \mathcal{W}^n, \quad n \geq 2
\end{aligned}$$

with $\tilde{f}(t)$, which has been defined in (2.5), denoting the linear approximation of $f(t)$.

## 5. A Posteriori Error Estimates of the Quadratic Reconstruction

In this section, we derive a posteriori error estimates for the method (2.2) by using the reconstructions (4.1) and (4.5).

Taking in (4.4) and (4.8) the inner product with $\widehat{E}(t)$, we can obtain, for $t \in I_n, n \geq 1$,

$$\left(\partial_t^\alpha \widehat{E}(t), \widehat{E}(t)\right) + \left(AE(t), \widehat{E}(t)\right) = \left(R_n(t), \widehat{E}(t)\right). \tag{5.1}$$

Using the relations

$$\left(\partial_t^\alpha \widehat{E}(t), \widehat{E}(t)\right) \geq \frac{1}{2} \partial_t^\alpha \|\widehat{E}(t)\|^2,$$

and

$$\begin{aligned}
\left(AE(t), \widehat{E}(t)\right) &= \frac{1}{2} \left(\|\widehat{E}(t)\|_1^2 + \|E(t)\|_1^2 - \|\widehat{E}(t) - E(t)\|_1^2\right) \\
&= \frac{1}{2} \left(\|\widehat{E}(t)\|_1^2 + \|E(t)\|_1^2 - \|U(t) - \widehat{U}(t)\|_1^2\right),
\end{aligned}$$

from (5.1), we get

$$\partial_t^\alpha \|\widehat{E}(t)\|^2 + \|\widehat{E}(t)\|_1^2 + \|E(t)\|_1^2 \le \|U(t) - \widehat{U}(t)\|_1^2 + 2\big(R_n(t), \widehat{E}(t)\big). \tag{5.2}$$

Now the $L^2_\alpha(0,T;V)$ error bounds can be formulated as the following theorem.

**Theorem 5.1 ($L^2_\alpha(0,T;V)$ Error Estimate).** *Let $U(t)$ be the* L1 *approximation to the solution of problem* (1.3), *$\widehat{U}$ be the corresponding reconstruction of $U$ defined in* (4.1) *and* (4.5), *$E = u - U$ and $\widehat{E} = u - \widehat{U}$. Then the following a posteriori error estimate is valid, for $t \in I_n, n \ge 1$,*

$$\begin{aligned} \frac{1}{3}\|\widehat{U} - U\|^2_{L^2_\alpha(0,t;V)} &\le \|\widehat{E}(t)\|^2 + \|E\|^2_{L^2_\alpha(0,t;V)} + \frac{1}{2}\|\widehat{E}\|^2_{L^2_\alpha(0,t;V)} \\ &\le \|E(0)\|^2 + \|\widehat{U} - U\|^2_{L^2_\alpha(0,t;V)} + 2\|R_n\|^2_{L^2_\alpha(0,t;V^*)}. \end{aligned} \tag{5.3}$$

*Proof.* We first show the upper bound. It follows from (5.2) that

$$\partial_t^\alpha \|\widehat{E}(t)\|^2 + \|E(t)\|_1^2 + \frac{1}{2}\|\widehat{E}(t)\|_1^2 \le \|U(t) - \widehat{U}(t)\|_1^2 + 2\|R_n(t)\|_{-1}^2, \tag{5.4}$$

where the Cauchy-Schwarz inequality has been used. Applying the integral operator $\partial_t^{-\alpha}$ to both sides of (5.4) yields

$$\begin{aligned} &\|\widehat{E}(t)\|^2 + \|E\|^2_{L^2_\alpha(0,t;V)} + \frac{1}{2}\|\widehat{E}\|^2_{L^2_\alpha(0,t;V)} \\ &\le \|\widehat{E}(0)\|^2 + \|\widehat{U} - U\|^2_{L^2_\alpha(0,t;V)} + 2\|R_n\|^2_{L^2_\alpha(0,t;V^*)}. \end{aligned}$$

With $\widehat{E}(0) = E(0)$, we thus easily obtain the desired upper bound.

We now turn to estimate the lower bound. In view of

$$\|\widehat{U}(s) - U(s)\|_1 \le \|E(s)\|_1 + \|\widehat{E}(s)\|_1,$$

we have

$$\|\widehat{U}(s) - U(s)\|_1^2 \le 3\left(\|E(s)\|_1^2 + \frac{1}{2}\|\widehat{E}(s)\|_1^2\right). \tag{5.5}$$

Apply the integral operator $\partial_t^{-\alpha}$ to both sides of (5.5) to obtain the desired lower bound. Hence the statements in theorem are proved. □

From (5.3), we can obtain the $L^\infty(0,t;H)$ estimate: For any $t \in I_n$,

$$\max_{0\le s\le t} \|\widehat{E}(s)\|^2 \le \|E(0)\|^2 + \|\widehat{U} - U\|^2_{L^2_\alpha(0,t;V)} + 2\|R_n\|^2_{L^2_\alpha(0,t;V^*)}.$$

Considering $E(t_n) = \widehat{E}(t_n)$ at all nodes $t_0, t_1, \cdots, t_N$, we also have

$$\max_{0\le i\le n} \|E(t_i)\|^2 \le \|E(0)\|^2 + \|\widehat{U} - U\|^2_{L^2_\alpha(0,t_n;V)} + 2\|R_n\|^2_{L^2_\alpha(0,t_n;V^*)}.$$

In view of the inequality

$$\int_0^t \omega_\alpha(t-s)\left(\|E(s)\|_1^2 + \frac{1}{2}\|\widehat{E}(s)\|_1^2\right) ds \ge \omega_\alpha(t)\int_0^t \left(\|E(s)\|_1^2 + \frac{1}{2}\|\widehat{E}(s)\|_1^2\right) ds,$$

we have the following $L^2(0,t;V)$ error estimates, for $t \in I_n, n \ge 1$,

$$\begin{aligned} &\|\widehat{E}(t)\|^2 + \omega_\alpha(t)\left(\|E(t)\|^2_{L^2(0,t;V)} + \frac{1}{2}\|\widehat{E}(t)\|^2_{L^2(0,t;V)}\right) \\ &\le \|E(0)\|^2 + \|\widehat{U} - U\|^2_{L^2_\alpha(0,t;V)} + 2\|R_n\|^2_{L^2_\alpha(0,t;V^*)}. \end{aligned}$$

### 5.1. A posteriori error estimates for the first step integration

Applying Theorem 5.1 to the first step integration, we have the same estimate as (5.3) with

$$\begin{aligned}\widehat{U}(t) - U(t) = &-t\bar{\partial}U^1 - \frac{1}{\Gamma(\alpha+2)}t^{\alpha+1}A\bar{\partial}U^1 - \frac{1}{\Gamma(\alpha+1)}t^{\alpha}AU^0 \\ &+ \int_0^t \omega_\alpha(t-s)P_1 f(s)ds, \quad t \in I_1,\end{aligned}$$

and $R_1(t) = f(t) - P_1 f(t), t \in I_1$.

### 5.2. A posteriori error estimates for $n \geq 2$

When $n \geq 2$, from Theorem 5.1 we can also derive a posteriori error estimates for the error $E$ in several different norms. To test contribution of the different error terms in time discretization, however, we will split the error term $R_n(t)$ into three parts

$$R_n(t) = R_f(t) + R_I(t) - \mathcal{W}^n, \quad t \in I_n,$$

where $\mathcal{W}^n$ has been defined in (4.7), and $R_I(t)$ and $R_f(t)$ are, respectively, defined by

$$\begin{aligned}R_I(t) := &\sum_{j=1}^{n-1}\left[\left(\ell_{n,-1}a_j(t_{n-1}) + \ell_{n,1}a_j(t_n)\right) - a_j(t)\right]\bar{\partial}U^j \\ &+ \frac{t-t_{n-1}}{\Gamma(2-\alpha)}\left(k_n^{-\alpha} - (t-t_{n-1})^{-\alpha}\right)\bar{\partial}U^n, \\ R_f(t) := &\, f - \tilde{f}. \end{aligned} \tag{5.6}$$

Then we have the following error estimate.

**Theorem 5.2 ($L^2_\alpha(0,T;V)$ Error Estimate).** *Let $U(t)$ be the* L1 *approximation to the solution of problems* (1.3), *$\widehat{U}$ be the corresponding reconstruction of $U$ defined in* (4.1) *and* (4.5), *$E = u - U$ and $\widehat{E} = u - \widehat{U}$. Then the following a posteriori error estimate is valid for $t \in I_n, n \geq 1$,*

$$\begin{aligned}\frac{1}{5}\|\widehat{U} - U\|^2_{L^2_\alpha(0,t;V)} &\leq \|\widehat{E}(t)\|^2 + \|E\|^2_{L^2_\alpha(0,t;V)} + \frac{1}{4}\|\widehat{E}\|^2_{L^2_\alpha(0,t;V)} \\ &\leq \|E(0)\|^2 + \|\widehat{U} - U\|^2_{L^2_\alpha(0,t;V)} + 4\|R_I\|^2_{L^2_\alpha(0,t;V^*)} \\ &\quad + 4\|R_f\|^2_{L^2_\alpha(0,t;V^*)} + 4\|\mathcal{W}^n\|^2_{L^2_\alpha(0,t;V^*)}.\end{aligned} \tag{5.7}$$

*Proof.* It follows from (5.2) that

$$\begin{aligned}&\partial_t^\alpha\|\widehat{E}(t)\|^2 + \|E(t)\|_1^2 + \frac{1}{4}\|\widehat{E}(t)\|_1^2 \\ \leq &\|U(t) - \widehat{U}(t)\|_1^2 + 4\|R_I(t)\|^2_{-1} \\ &+ 4\|R_f(t)\|^2_{-1} + 4\|\mathcal{W}^n\|^2_{-1}.\end{aligned} \tag{5.8}$$

Applying the integral operator $\partial_t^{-\alpha}$ to both sides of (5.8) yields

$$\begin{aligned}&\|\widehat{E}(t)\|^2 + \|E\|^2_{L^2_\alpha(0,t;V)} + \frac{1}{4}\|\widehat{E}\|^2_{L^2_\alpha(0,t;V)} \\ \leq &\|\widehat{E}(0)\|^2 + \|\widehat{U} - U\|^2_{L^2_\alpha(0,t;V)} + 4\|R_I\|^2_{L^2_\alpha(0,t;V^*)} \\ &+ 4\|R_f\|^2_{L^2_\alpha(0,t;V^*)} + 4\|\mathcal{W}^n\|^2_{L^2_\alpha(0,t;V^*)},\end{aligned}$$

which implies the desired upper bound.

The low bound can be obtained by using a similar argument to (5.5). Thus, the proof is complete. □

From (5.7), we can obtain the $L^\infty(0,t;H)$ estimates: For any $t \in I_n$,

$$\begin{aligned}\max_{0\le s\le t}\|\widehat{E}(s)\|^2 &\le \|E(0)\|^2 + \|\widehat{U}-U\|^2_{L^2_\alpha(0,t;V)} + 4\|R_I\|^2_{L^2_\alpha(0,t;V^*)} \\ &\quad + 4\|R_f\|^2_{L^2_\alpha(0,t;V^*)} + 4\|\mathcal{W}^n\|^2_{L^2_\alpha(0,t;V^*)}, \\ \max_{0\le i\le n}\|E(t_i)\|^2 &\le \|E(0)\|^2 + \|\widehat{U}-U\|^2_{L^2_\alpha(0,t_n;V)} + 4\|R_I\|^2_{L^2_\alpha(0,t_n;V^*)} \\ &\quad + 4\|R_f\|^2_{L^2_\alpha(0,t_n;V^*)} + 4\|\mathcal{W}^n\|^2_{L^2_\alpha(0,t_n;V^*)}.\end{aligned}$$

In view of the inequality (1.2), we have the following $L^2(0,T;V)$ error estimate.

**Corollary 5.1 ($L^2(0,T;V)$ Error Estimate).** *Let $U(t)$ be the* L1 *approximation to the solution of problems* (1.3)*, $\widehat{U}$ be the corresponding reconstruction of $U$ defined in* (4.1) *and* (4.5)*, $E = u - U$ and $\widehat{E} = u - \widehat{U}$. Then the following a posteriori error estimate is valid, for $t \in I_n, n \ge 1$,*

$$\begin{aligned}\frac{\omega_\alpha(t)}{5}\|\widehat{U}-U\|^2_{L^2(0,t;V)} &\le \|\widehat{E}(t)\|^2 + \omega_\alpha(t)\|E\|^2_{L^2(0,t;V)} + \frac{\omega_\alpha(t)}{4}\|\widehat{E}\|^2_{L^2(0,t;V)} \\ &\le \|E(0)\|^2 + \|\widehat{U}-U\|^2_{L^2_\alpha(0,t;V)} + 4\|R_I\|^2_{L^2_\alpha(0,t;V^*)} \\ &\quad + 4\|R_f\|^2_{L^2_\alpha(0,t;V^*)} + 4\|\mathcal{W}^n\|^2_{L^2_\alpha(0,t;V^*)}.\end{aligned}$$

We conclude this section with a remark about our results. Using (4.5) and (5.6), when $f$ is sufficiently smooth we can easily show that the terms $\|\widehat{U}-U\|^2_{L^2_\alpha(0,t;V)}$ and $\|R_f\|_{L^2_\alpha(0,t_n;V^*)}$ in error estimates are of order 2. This means that their orders are higher than the error order $2-\alpha$ of the L1 scheme. It is also easy to show that the term $\|R_I\|^2_{L^2_\alpha(0,t;V^*)}$ is of optimal order $2-\alpha$ because

$$R_I = \big(\ell_{n,-1}\bar{\partial}_t^\alpha U^{n-1} + \ell_{n,1}\bar{\partial}_t^\alpha U^n\big) - \partial_t^\alpha U(t),$$

which is a linear interpolation approximation. As for the term $\|\mathcal{W}^n\|^2_{L^2_\alpha(0,t;V^*)}$, from (4.6), we get

$$\mathcal{W}^n = \partial_t^\alpha \widehat{U}(t) - \partial_t^\alpha U(t) = \partial_t^\alpha\big(\widehat{U}(t) - U(t)\big),$$

and therefore it is of optimal order $2-\alpha$.

## 6. Numerical Experiments: Uniform Partition

Using several numerical examples, we now illustrate the theoretical results of the previous sections. It is worthwhile to note that the theoretical results obtained in this paper are valid for the 2D and 3D problems, although we consider only 1D example here. We study the effectivity indices corresponding to the error estimators on several test cases with both smooth and nonsmooth solutions.

Let us define the estimators

$$\begin{aligned}&\mathcal{E}_U := \|\widehat{U}-U\|_{L^2_\alpha(0,T;V)}, \quad \mathcal{E}_f := \|R_f\|_{L^2_\alpha(0,T;V^*)}, \\ &\mathcal{E}_I := \|R_I\|_{L^2_\alpha(0,T;V^*)}, \qquad \mathcal{E}_W := \|\mathcal{W}^n\|_{L^2_\alpha(0,T;V^*)}.\end{aligned}$$

We denote by $\mathrm{Err}_m$ the discrete maximum norm in time of $E$, i.e.

$$\mathrm{Err}_m = \max_{1\le n\le N} \|E(t_n)\| = \max_{1\le n\le N} \|\widehat{E}(t_n)\|,$$

by $\mathrm{Err}_T$ the error at time $T$, i.e.

$$\mathrm{Err}_T = \|E(T)\| = \|E(t_N)\|,$$

and by $\mathrm{Err}_{1\alpha}$ the $L^2_\alpha(0,T;V)$-norm of the error, i.e. $\mathrm{Err}_{1\alpha} = \|E\|_{L^2_\alpha(0,T;V)}$. The lower and upper estimators are $\mathcal{E}_U/5$ and $\mathcal{E}_U + 4\mathcal{E}_f + 4\mathcal{E}_I + 4\mathcal{E}_W$, respectively, see (5.7). We are also interested in computing the effectivity indices $ei_L$ and $ei_U$, defined as

$$ei_L := \frac{\text{Lower estimator}}{(5/4)\mathrm{Err}_{1\alpha}}, \quad ei_U := \frac{\text{Upper estimator}}{\mathrm{Err}_T + (5/4)\mathrm{Err}_{1\alpha}},$$

respectively. Note that since $\|\widehat{E}\|_{L^2_\alpha(0,T;V)}$ is a higher order term than $\|E\|_{L^2_\alpha(0,T;V)}$, the error $\|E\|_{L^2_\alpha(0,T;V)} + (1/4)\|\widehat{E}\|_{L^2_\alpha(0,T;V)}$ is approximated by the error $(5/4)\mathrm{Err}_{1\alpha}$ in computing the effectivity indices $ei_L$ and $ei_U$.

We proceed by studying two different cases. The first one concerns problem which has a smooth solution, while in the second one we consider (1.3) with a nonsmooth solution.

**Example 6.1 (Smooth Solution).** Let us still consider the problem (3.6) with the exact solution

$$u(x,t) = (1+t^2)x(1-x).$$

The true error $\mathrm{Err}_m$, and the a posteriori error estimators $\mathcal{E}_U, \mathcal{E}_f, \mathcal{E}_I, \mathcal{E}_W$, as well as their temporal convergence orders are listed in Tables 6.1 and 6.2, respectively. From these numerical results, we observe that the true error $\mathrm{Err}_m$ and the a posteriori error estimators $\mathcal{E}_I, \mathcal{E}_W$ are of optimal order $2-\alpha$. The a posteriori error quantities $\mathcal{E}_U$ and $\mathcal{E}_f$ are of optimal order 2.

From Table 6.2, we can see that the effectivity index $ei_L$ depends on $\alpha$, and the effectivity index $ei_U$ is around 4.4 for all three cases.

Table 6.1: Example 6.1: The errors and their convergence orders of L1 method (2.2) for (3.6), where $T = 1$ and $M = 512$.

| $\alpha$ | $N$ | $\mathrm{Err}_m$ | Order | $\mathcal{E}_U$ | Order | $\mathcal{E}_f$ | Order |
|---|---|---|---|---|---|---|---|
| 0.25 | 16 | 2.9585E-05 | - | 3.6846E-04 | - | 4.0675E-04 | - |
| | 32 | 9.2304E-06 | 1.6804 | 9.5129E-05 | 1.9535 | 1.0445E-04 | 1.9613 |
| | 64 | 2.8527E-06 | 1.6940 | 2.4362E-05 | 1.9652 | 2.6679E-05 | 1.9690 |
| | 128 | 8.7525E-07 | 1.7045 | 6.2057E-06 | 1.9729 | 6.7866E-06 | 1.9749 |
| 0.5 | 16 | 1.2098E-04 | - | 4.2338E-04 | - | 4.6169E-04 | - |
| | 32 | 4.3485E-05 | 1.4762 | 1.0692E-04 | 1.9853 | 1.1659E-04 | 1.9854 |
| | 64 | 1.5551E-05 | 1.4835 | 2.6915E-05 | 1.9901 | 2.9357E-05 | 1.9896 |
| | 128 | 5.5421E-06 | 1.4884 | 6.7603E-06 | 1.9932 | 7.3771E-06 | 1.9925 |
| 0.75 | 16 | 3.9180E-04 | - | 4.4976E-04 | - | 4.6005E-04 | - |
| | 32 | 1.6542E-04 | 1.2439 | 1.1031E-04 | 2.0275 | 1.1586E-04 | 1.9893 |
| | 64 | 6.9720E-05 | 1.2465 | 2.7259E-05 | 2.0168 | 2.9172E-05 | 1.9897 |
| | 128 | 2.9355E-05 | 1.2479 | 6.7675E-05 | 2.0100 | 7.3499E-06 | 1.9888 |

Table 6.2: Example 6.1: The errors with their orders, and the effecitvity indices of error estimators of L1 method (2.2) for (3.6), where $T = 1$ and $M = 512$.

| $\alpha$ | $N$ | $\mathcal{E}_I$ | Order | $\mathcal{E}_W$ | Order | $ei_L$ | $ei_U$ |
|---|---|---|---|---|---|---|---|
| 0.25 | 16 | 9.1929E-05 | - | 7.6227E-05 | - | 0.1310 | 4.5071 |
| | 32 | 3.0001E-05 | 1.6155 | 2.2188E-05 | 1.7805 | 0.1260 | 4.5057 |
| | 64 | 9.5901E-06 | 1.6453 | 6.4390E-06 | 1.7848 | 0.1202 | 4.4998 |
| | 128 | 3.0201E-06 | 1.6669 | 1.8674E-06 | 1.7857 | 0.1138 | 4.4909 |
| 0.5 | 16 | 4.2709E-04 | - | 2.1441E-04 | - | 0.0868 | 4.4127 |
| | 32 | 1.5780E-04 | 1.4364 | 7.3420E-05 | 1.5461 | 0.0717 | 4.3872 |
| | 64 | 5.7444E-05 | 1.4579 | 2.5297E-05 | 1.5371 | 0.0575 | 4.3577 |
| | 128 | 2.0715E-05 | 1.4714 | 8.7708E-06 | 1.5282 | 0.0449 | 4.3282 |
| 0.75 | 16 | 1.3914E-03 | - | 6.2937E-04 | - | 0.0456 | 4.3876 |
| | 32 | 6.0038E-04 | 1.2126 | 2.6375E-04 | 1.2547 | 0.0292 | 4.3788 |
| | 64 | 2.5613E-04 | 1.2289 | 1.1058E-04 | 1.2541 | 0.0182 | 4.3710 |
| | 128 | 1.0859E-04 | 1.2379 | 4.6396E-05 | 1.2530 | 0.0111 | 4.3648 |

**Example 6.2 (Nonsmooth Solution).** In the second experiment we consider (3.6) with a nonsmooth exact solution

$$u(x,t) = (1 + t^{\alpha})x(1 - x).$$

The true errors $\mathrm{Err}_m, \mathrm{Err}_{1\alpha}, \mathcal{E}_U$, and their convergence orders are presented in Table 6.3. The a posteriori error estimators $\mathcal{E}_f, \mathcal{E}_I, \mathcal{E}_W$, and their temporal convergence orders are listed in Table 6.4. From these numerical results, we observe that a posteriori error quantities $\mathcal{E}_U$ and $\mathcal{E}_f$ are still of order 2. The former illustrates that the quadratic reconstruction $\widehat{U}$ is a higher order approximation of $U$ and the difference between them is independent of the regularity of the exact solution $u$, and the latter confirms the error behaviour of the linear interpolation for $f$ when it is sufficiently smooth. Observe also that the true error $\mathrm{Err}_m, \mathrm{Err}_{1\alpha}$ and the posteriori error estimators $\mathcal{E}_I, \mathcal{E}_W$ are only of $\alpha$ order. These numerical results show that the $L1$ method with nonsmooth data is only convergent of order $\alpha$ on the uniform mesh, which is in accordance with the result of initial singularity.

Table 6.3: Example 6.2: The exact errors and their convergence orders of L1 method (2.2) for (3.6), where $T = 1$ and $M = 512$.

| $\alpha$ | $N$ | $\mathrm{Err}_m$ | Order | $\mathrm{Err}_{1\alpha}$ | Order | $\mathcal{E}_U$ | Order |
|---|---|---|---|---|---|---|---|
| 0.25 | 16 | 7.4328E-04 | - | 6.5266E-03 | - | 7.5322E-03 | - |
| | 32 | 6.2481E-04 | 0.2505 | 5.4453E-03 | 0.2613 | 1.7481E-03 | 2.1073 |
| | 64 | 5.2519E-04 | 0.2506 | 4.5403E-03 | 0.2622 | 4.0825E-04 | 2.0982 |
| | 128 | 4.4414E-04 | 0.2506 | 3.7818E-03 | 0.2637 | 9.8960E-05 | 2.0455 |
| 0.5 | 16 | 4.6297E-04 | - | 7.3705E-03 | - | 1.0696E-03 | - |
| | 32 | 3.2399E-04 | 0.5149 | 5.0945E-03 | 0.5328 | 2.5038E-04 | 2.0936 |
| | 64 | 2.2638E-04 | 0.5171 | 3.5182E-03 | 0.5341 | 5.8995E-05 | 2.0854 |
| | 128 | 1.5801E-04 | 0.5187 | 2.4277E-03 | 0.5352 | 1.4323E-05 | 2.0421 |
| 0.75 | 16 | 4.3779E-04 | - | 8.8184E-03 | - | 1.9029E-03 | - |
| | 32 | 2.5459E-04 | 0.7820 | 4.9823E-03 | 0.8237 | 4.4585E-04 | 2.0935 |
| | 64 | 1.4701E-04 | 0.7922 | 2.8128E-03 | 0.8248 | 1.0793E-04 | 2.0463 |
| | 128 | 8.4859E-05 | 0.7928 | 1.5871E-03 | 0.8256 | 2.6539E-05 | 2.0240 |

Table 6.4: Example 6.2: The a posteriori errors and their orders of L1 method (2.2) for (3.6), where $T = 1$ and $M = 512$.

| $\alpha$ | $N$ | $\mathcal{E}_f$ | Order | $\mathcal{E}_I$ | Order | $\mathcal{E}_W$ | Order |
|---|---|---|---|---|---|---|---|
| 0.25 | 16 | 8.0505E-04 | - | 3.4492E-03 | - | 1.2272E-03 | - |
| | 32 | 2.0978E-04 | 1.9402 | 2.9069E-03 | 0.2467 | 1.0345E-03 | 0.2468 |
| | 64 | 5.4151E-05 | 1.9424 | 2.4304E-03 | 0.2582 | 8.7181E-04 | 0.2579 |
| | 128 | 1.3884E-05 | 1.9579 | 2.0208E-03 | 0.2662 | 7.2647E-04 | 0.2631 |
| 0.5 | 16 | 7.0582E-04 | - | 2.5685E-03 | - | 8.1450E-04 | - |
| | 32 | 1.7902E-04 | 1.9791 | 1.7727E-03 | 0.5349 | 5.7649E-04 | 0.4986 |
| | 64 | 4.5199E-05 | 1.9857 | 1.2402E-03 | 0.5154 | 4.0475E-04 | 0.5102 |
| | 128 | 1.1376E-05 | 1.9901 | 8.7393E-04 | 0.5049 | 2.8337E-04 | 0.5143 |
| 0.75 | 16 | 5.5627E-04 | - | 1.1583E-03 | - | 8.7355E-04 | - |
| | 32 | 1.3958E-04 | 1.9946 | 6.9054E-04 | 0.7462 | 5.2141E-04 | 0.7447 |
| | 64 | 3.4983E-05 | 1.9963 | 4.0954E-04 | 0.7537 | 3.0857E-04 | 0.7568 |
| | 128 | 8.7617E-06 | 1.9973 | 2.4161E-04 | 0.7613 | 1.8181E-04 | 0.7631 |

## 7. Numerical Experiments: Adaptivity

From the above numerical experiments, we know that the optimal convergence order of numerical algorithm with nonsmooth data couldn't be achieved on the uniform mesh. In this section, in order to deal with the nonsmooth case, we develop a time adaptive algorithm for TFPDEs using barrier function [25–27]. Inspired by [26], we choose the similar barrier function to obtain the optimal results.

**Theorem 7.1.** *Let the operator $A$ in* (1.3)*, for some $\lambda \in \mathbb{R}$, satisfy $(Av, v) \geq \lambda\|v\|^2$, $\forall\, v \in V$. Suppose a unique solution $u$ of* (1.3) *and its approximation $\widehat{U}$ are in $L^\infty(0, t; H) \cap W^{1,\infty}(\epsilon, t; H)$ for any $0 < \epsilon < t \leq T$, and also in $V$ for any $t > 0$, while $R_h(t) = R_n(t) + A(U - \widehat{U})$. Then*

$$\|(u - \widehat{U})(t)\| \leq (\partial_t^\alpha + \lambda)^{-1}\|R_h(t)\|, \quad t > 0.$$

*Proof.* Adding the term $A(\widehat{U} - U)$ into the Eq. (4.8) and using the condition $(Av, v) \geq \lambda\|v\|^2$, we can obtain the theorem, which is similar to [26, Theorem 2.2]. □

From the result of Theorem 7.1, if the barrier function $\mathcal{E}(t)$ satisfies

$$\|R_h(t)\| \leq \big(\partial_t^\alpha + \lambda\big)\mathcal{E}(t),$$

we can obtain the result of pointwise-in-time error $\|\widehat{E}(t)\| \leq \mathcal{E}(t)$, $\forall\, t \geq 0$, which is desirable for the theoretical analysis and numerical experiments. But the barrier function $\mathcal{E}(t)$ must ensure the limit condition $(\partial_t^\alpha + \lambda)\mathcal{E}(t) > 0, t > 0$, which is not satisfied for most barrier function $\mathcal{E}(t)$. Thanks to the [26], we take two barrier functions $\mathcal{E}(t)$ at the following lemma, which are appropriate for our goal.

**Lemma 7.1 ([26]).** *Under the conditions of Theorem* 7.1 *with $\lambda \geq 0$, for the error $\widehat{E}(t)$ one has*

$$\|\widehat{E}(t)\| \leq \sup_{0<s\leq t}\left\{\frac{\|R_h(s)\|}{\mathcal{R}_0(s)}\right\}, \quad \|\widehat{E}(t)\| \leq t^{\alpha-1}\sup_{0<s\leq t}\left\{\frac{\|R_h(s)\|}{\mathcal{R}_1(s)}\right\},$$

*where*

$$\mathcal{R}_0(t) := \Gamma^{-1}(1-\alpha)t^{-\alpha} + \lambda, \quad \mathcal{R}_1(t) := \Gamma^{-1}(1-\alpha)t^{-1}\rho(\tau/t) + \lambda\mathcal{E}_1(t),$$
$$\mathcal{E}_1(t) := \max\{\tau, t\}^{\alpha-1}, \qquad \rho(s) := s^{\alpha-1}\big[1 - \big((1-s)^+\big)^{1-\alpha}\big].$$

### 7.1. The adaptive algorithm

We briefly describe our adaptive algorithm used here. Let Tol denote the tolerance such that $\|\mathcal{R}_h(t)\| \leq$Tol$*\mathcal{R}_p(t), p=0,1$. In order to characterize $t \in (t_{n-1}, t_n)$ in the actual calculation, we have to take $GN$ points on the interval $(t_{n-1}, t_n)$ to check $\|\mathcal{R}_h(t_k)\| \leq \text{Tol} * \mathcal{R}_p(t_k), k = 1, 2, \ldots, GN$. The main steps of the time adaptive algorithm are summarized schematically in the pseudocode below. More precisely, the adaptive algorithm starts by advancing the solution and computing the time estimator $\|\mathcal{R}_h(t)\|$ and $\mathcal{R}_p(t)$. Based on the time estimator $\|\mathcal{R}_h(t)\|$ and $\mathcal{R}_p(t)$, we could perform time-step refinement and time-step coarsening as needed.

Reasonable choices for the parameters $Q = 1.1$, while for $p = 0$ and $p = 1$ we take $\tau^* = 5\text{Tol}^{1/\alpha}$ and $\tau^* = \text{Tol}$.

**Algorithm 7.1:** Time Adaptive Algorithm.

```
Choose Parameters: Tol, GN, Q.
Initialization: U^0, t_0 = 0, k_1 = τ*, n = 0.
while t_n < T do
    Set flag = 2.
    while flag > 0 do
        if flag == 1 then
            k_n = k_n/Q.
        end
        Set t_n := t_{n-1} + k_n.
        Solve the discrete problem: {U^j}_{j=0}^{n-1} → {U^j}_{j=0}^{n} .
        Insert GN points evenly on the interval (t_{n-1}, t_n).
        Set k = 1, Count = 0.
        while k <= GN do
            Compute Estimator ||R_h(t_k)||, R_p(t_k).
            if ||R_h(t_k)|| > Tol * R_p(t_k) then
                break.
            else
                Count = Count + 1.
            end
            k = k + 1.
        end
        if Count == GN then
            flag = 0, k_n = k_n * Q.
        else
            flag = 1.
        end
    end
    Let n = n + 1.
    if t_n == T then
        break.
    end
end
```

### 7.2. Numerical experiments

To visually compare with the previous numerical experiments, we still consider the problem in Example 6.2 but use the adaptive algorithm, which could be applied to both 2D and 3D examples. Firstly, we discuss the case of the barrier function $\mathcal{R}_0(t)$ in Fig. 7.1. We observe the estimators $\|\widehat{E}(t)\|$ and $\|R_n(t)\|_{L^2_\alpha(0,T;V^*)}$, which are plotted in Fig. 7.1, are optimal convergence rates of $2-\alpha$ when $\alpha = 0.4, 0.8$. We also observe that adaptive mesh is more dense at initial time and more sparse at terminal time than graded mesh, which is reasonable for the problem with nonsmooth data. Then we discuss the adaptive algorithm with barrier function $\mathcal{R}_1(t)$ in Fig. 7.2. We observe that the estimators $\|\widehat{E}(T)\|$ and $\|R_n(t)\|_{L^2_\alpha(0,T;V^*)}$ on the adaptive mesh achieve the optimal convergence rates of $2-\alpha$ when $\alpha = 0.3$ and $\alpha = 0.7$. And the pointwise error $\|\widehat{E}(t_n)\|$ on the adaptive mesh is compared with error on the nonuniform $\mathrm{Tol}\cdot t^{\alpha-1}$.

Comparison of the numerical results in this section and numerical results in Example 6.2 suggests that nonuniform mesh could improve the convergence which is influenced by the initial singularity of nonsmooth problem. This means that adaptive algorithm is necessary to

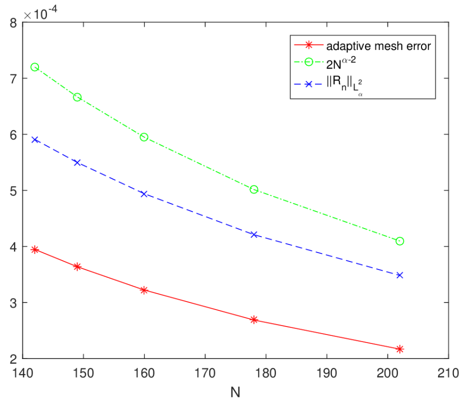


(a) $\alpha = 0.4$

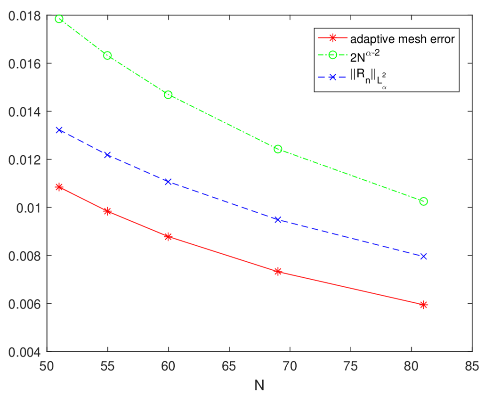


(b) $\alpha = 0.8$

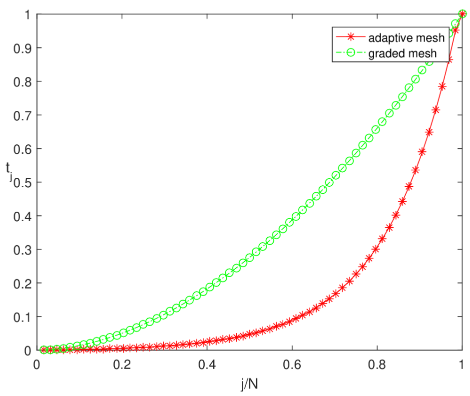


(c) $\{t_j\}_{j=0}^N$ as a function of $j/N$

Fig. 7.1. Adaptive algorithm with $\mathcal{R}_0(t)$ for Example 6.2: Estimators $\max_{[0,T]}\|\widehat{E}(t)\|, \|R_n(t)\|_{L^2_\alpha(0,T;V^*)}$ and reference estimator $2N^{\alpha-2}$ on the adaptive mesh, where $\alpha = 0.4$ (upper left) and $\alpha = 0.8$ (upper right). Lower: graphs of $\{t_j\}_{j=0}^N$ as a function of $j/N$ for the adaptive mesh and graded mesh with $\gamma = (2-\alpha)/\alpha, \alpha = 0.7, \mathrm{Tol} = 10^{-3}, N = 63$.

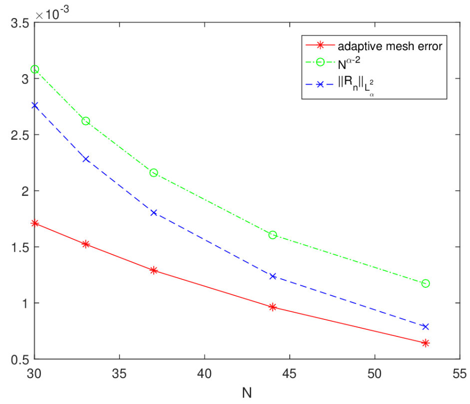


(a) $\alpha = 0.3$

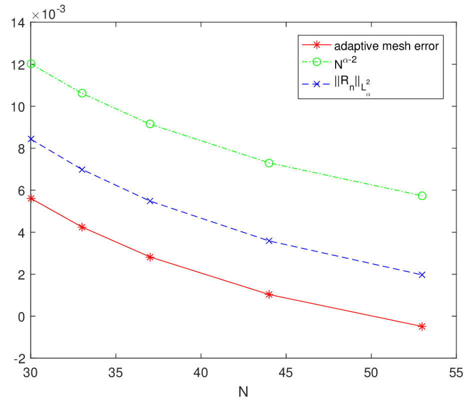


(b) $\alpha = 0.7$

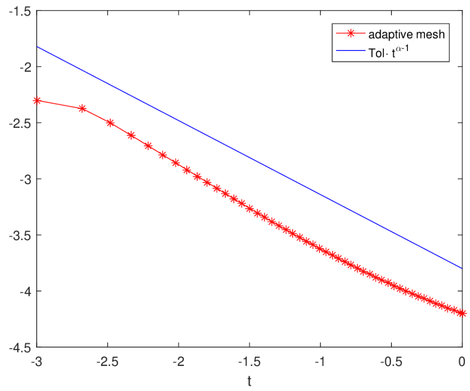


(c) log-log graphs of pointwise error $\|\widehat{E}(t_j)\|$

Fig. 7.2. Adaptive algorithm with $\mathcal{R}_1(t)$ for Example 6.2: Estimators $\max_{[0,T]} \|\widehat{E}(t)\|$, $\|R_n(t)\|_{L^2_\alpha(0,T;V^*)}$ and reference estimator $N^{\alpha-2}$ on the adaptive mesh, where $\alpha = 0.3$ (upper left) and $\alpha = 0.7$ (upper right). Lower: log-log graphs of pointwise error $\|\widehat{E}(t_j)\|$ on the adaptive mesh and nonuniform mesh $\mathrm{Tol} \cdot t^{\alpha-1}$ with $\alpha = 0.4, \mathrm{Tol} = 10^{-3}, N = 49$.

constructing numerical algorithm for nonsmooth problem. Thanks to the adaptive algorithm, quadratic reconstruction for the $L1$ method could achieve the optimal order no matter whether the initial data is smooth or not.

We also note that a posteriori error estimator of the linear reconstruction, which has been discussed with smooth data in the Section 3, can also obtain optimal convergence rate for nonsmooth problem on an adaptive mesh in [26]. Thus it is interesting to compare the computational efficiency and accuracy of a posteriori error estimator between the linear reconstruction and the quadratic reconstruction. These are done in Figs. 7.3-7.4.

As can be seen from Figs. 7.3 and 7.4, the true error of the adaptive algorithm based on quadratic reconstruction is smaller than that of linear reconstruction, regardless of whether $\mathcal{R}_0(t)$ or $\mathcal{R}_1(t)$ is used. Compared with the adaptive algorithm based on linear reconstruction, the computation time of the adaptive algorithm based on quadratic reconstruction using $\mathcal{R}_0(t)$ is not much different, while the computation time using $\mathcal{R}_1(t)$ is significantly less. Therefore, it is meaningful to use the technique based on the quadratic reconstruction of the numerical solution for a posteriori error estimates.

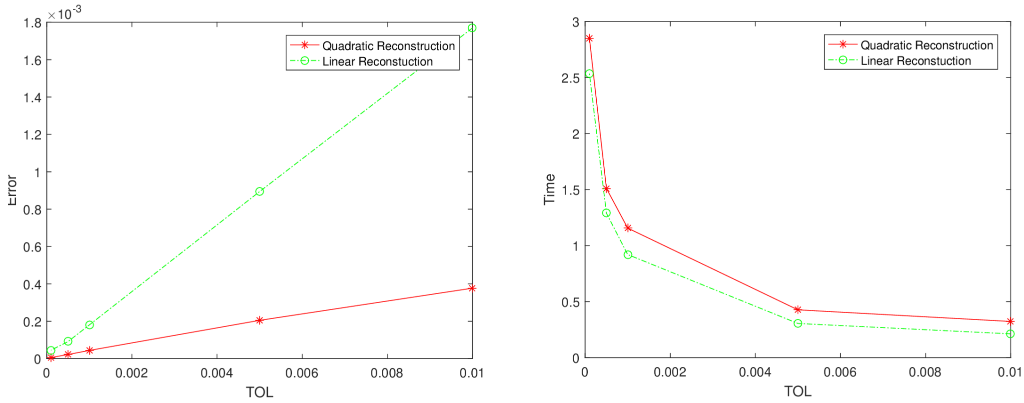


Fig. 7.3. Adaptive algorithm with $\mathcal{R}_0(t)$ in Example 6.2: A posteriori error estimator $\max_{[0,T]} \|E(t)\|$ of the linear reconstruction and a posteriori error estimator $\max_{[0,T]} \|\widehat{E}(t)\|$ of the quadratic reconstruction on the adaptive mesh when $\alpha = 0.5$ (left) and the corresponding computation time (right).

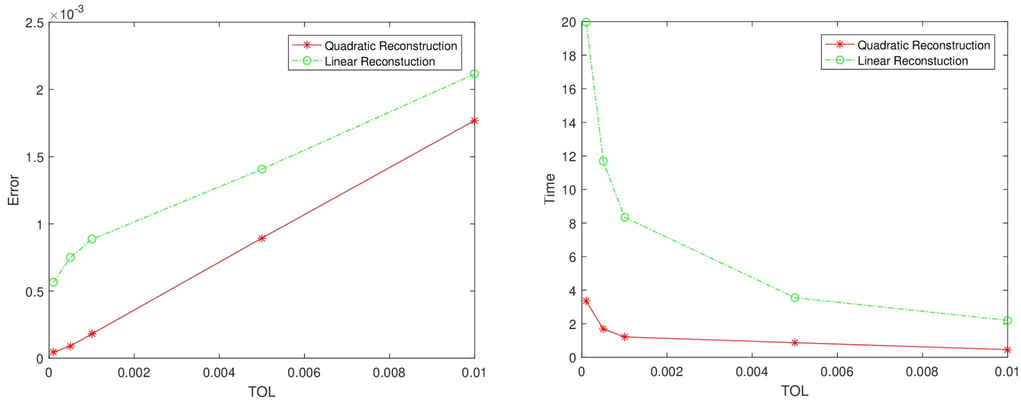


Fig. 7.4. Adaptive algorithm with $\mathcal{R}_1(t)$ in Example 6.2: A posteriori error estimator $\max_{[0,T]} \|E(t)\|$ of the linear reconstruction and a posteriori error estimator $\max_{[0,T]} \|\widehat{E}(t)\|$ of the quadratic reconstruction on the adaptive mesh when $\alpha = 0.5$ (left) and the corresponding computation time (right).

## 8. Concluding Remarks

In this paper, we derived optimal order a posteriori error estimates for the L1 time discretization method for TFPDEs. In view of the weak regularity of the solutions to this class of equations, a posteriori error estimates are extremely important for solving adaptively TFPDEs. Firstly, we derived a posteriori error estimate of the linear reconstruction, which is suboptimal order with respect to the uniform step-size by the L1 method even for the problem with smooth solution. To derive optimal order a posteriori error estimates, we introduced fractional integral reconstruction for the first-step integration and continuous, piecewise quadratic time reconstructions $\widehat{U}(t)$ on the rest integration intervals for the L1 method. By means of quadratic reconstructions, we obtain the upper error bounds in the $L^2_\alpha(0,t;V)$-, $L^2(0,t;V)$- and $L^\infty(0,t;H)$-norms as well as the upper and lower error bounds in the $L^2_\alpha(0,t;V)$- and $L^2(0,T;V)$-norms. It is worth emphasizing that these bounds depend only upon the discretization parameters and the data of problems and thus are computable. Numerical Example 6.1

show that the true error and a posteriori error estimators are of optimal order $2-\alpha$ for the problem with smooth solution, but numerical Example 6.2 indicate that using uniform mesh could only achieve convergence of $\alpha$ order for the problem with nonsmooth data. Based on the technique of barrier function, we developed a time adaptive algorithm. Then we perform the numerical Example 6.2 again on the adaptive mesh and check that the true error and a posteriori error estimators recover the optimal convergence, which can be seen in Figs. 7.1 and 7.2. Thus numerical results confirm the theoretical analysis and reveal the effectiveness of the a posteriori error estimates and the time adaptive algorithm no matter whether the initial data is smooth or nonsmooth. Finally, from the error and computation time of the adaptive algorithm, which has been shown in Figs. 7.3 and 7.4, we can know that the adaptive algorithm based on the quadratic reconstruction is more effective than the adaptive algorithm based on the linear reconstruction.

In this paper, we only considered the a posteriori error estimates for time discretization methods but not for the space discretization methods. Deriving a posteriori error estimates for fully discrete approximations for TFPDEs will be our future work.

**Acknowledgments.** The authors would like to thank the referees for comments and suggestions that led to improvements in the presentation of this paper.

This work was supported by the Natural Science Foundation of China (Grants 12271367, 12071403), by the Shanghai Science and Technology Planning Projects (Grant 20JC1414200).

## References

[1] G. Akrivis, C. Makridakis, and R.H. Nochetto, A posteriori error estimates for the Crank-Nicolson method for parabolic equations, *Math. Comp.*, **75** (2006), 511–531.

[2] A.A. Alikhanov, A priori estimates for solutions of boundary value problems for fractional-order equations, *Differ. Equ.*, **46** (2010), 660–666.

[3] L. Banjai and M. López-Fernández, Efficient high order algorithms for fractional integrals and fractional differential equations, *Numer. Math.*, **141** (2019), 289–317.

[4] L. Banjai and C. Makridakis, A posteriori error analysis for approximations of time-fractional subdiffusion problems, *Math. Comp.*, **91** (2021), 1711–1737.

[5] E. Bänsch, F. Karakatsani, and C. Makridakis, A posteriori error control for fully discrete Crank-Nicolson schemes, *SIAM J. Numer. Anal.*, **50** (2012), 2845–2872.

[6] H. Brunner, L. Ling, and M. Yamamoto, Numerical simulations of 2D fractional subdiffusion problems, *J. Comput. Phys.*, **229** (2010), 6613–6622.

[7] W. Cao, F. Zeng, Z. Zhang, and G.E. Karniadakis, Implicit-explicit difference scheme for nonlinear fractional differential equations with nonsmooth solutions, *SIAM J. Sci. Comput.*, **38** (2016), A3070–A3093.

[8] H. Chen and M. Stynes, Error analysis of a second-order method on fitted meshes for a time-fractional diffusion problem, *J. Sci. Comput.*, **79** (2019), 624–647.

[9] X. Chen, F. Zeng, and G.E. Karniadakis, A tunable finite difference method for fractional differential equations with non-smooth solutions, *Comput. Methods Appl. Mech. Engrg.*, **318** (2017), 193–214.

[10] X. Cheng, H. Qin, and J. Zhang, A compact ADI scheme for two-dimensional fractional subdiffusion equation with Neumann boundary condition, *Appl. Numer. Math.*, **156** (2020), 50–62.

[11] K. Diethelm, An algorithm for the numerical solution of differential equations of fractional order, *Trans. Numer. Anal.*, **5** (1997), 1–6.

[12] K. Diethelm, J.M. Ford, N.J. Ford, and M. Weilbeer, Pitfalls in fast numerical solution of fractional differential equations, *J. Comput. Appl. Math.*, **186** (2006), 482–503.

[13] K. Diethelm, R. Garrappa, and M. Stynes, Good (and not so good) practices in computational methods for fractional calculus, *Mathematics*, **8** (2020), 324.

[14] N.J. Ford, J. Xiao, and Y. Yan, A finite element method for time-fractional partial differential equations, *Fract. Calc. Appl. Math.*, **14** (2011), 454–474.

[15] N.J. Ford, J. Xiao, and Y. Yan, Stability of a numerical method for a space-time-fractional telegraph equations, *Comput. Methods Appl. Math.*, **12** (2012), 454–474.

[16] G.H. Gao, Z.Z. Sun, and H.W. Zhang, A new fractional numerical differentialion formula to approximate the Caputo fractional derivative and its applications, *J. Comput. Phys.*, **259** (2014), 33–50.

[17] B. Jin, *Fractional Differential Equations*, Springer, 2021.

[18] B. Jin, R. Lazarov, and Z. Zhou, Two fully discrete schemes for fractional diffusion and diffusion-wave equations with nonsmooth data, *SIAM J. Sci. Comput.*, **38** (2016), A146–A170.

[19] B. Jin, R. Lazarov, and Z. Zhou, An analysis of the L1 scheme for the subdiffusion equation with nonsmooth data, *IMA J. Numer. Anal.*, **36** (2016), 197–221.

[20] B. Jin, R. Lazarov, and Z. Zhou, Numerical methods for time-fractional evolution equations with nonsmooth data: A concise overview, *Comput. Methods Appl. Mech. Engrg.*, **346** (2019), 332–358.

[21] B. Jin, B. Li, and Z. Zhou, Correction of high-order BDF convolution quadrature for fractional evolution equations, *SIAM J. Sci. Comput.*, **39** (2017), A3129–A3152.

[22] B. Jin, B. Li, and Z. Zhou, An analysis of the Crank-Nicolson method for subdiffusion, *IMA J. Numer. Anal.*, **38** (2018), 518–541.

[23] B. Jin, B. Li, and Z. Zhou, Subdiffusion with time-dependent coefficients: Improved regularity and second-order time stepping, *Numer. Math.*, **145** (2020), 883–913.

[24] A.A.A. Kilbas, H.M. Srivastava, and J.J. Trujillo, *Theory and Applications of Fractional Differential Equations*, in: *North-Holland Mathematics Studies*, Vol. 204, 2006.

[25] N. Kopteva, Error analysis of the L1 method on graded and uniform meshes for a fractional-derivative problem in two and three dimensions, *Math. Comp.*, **88** (2019), 2135–2155.

[26] N. Kopteva, Pointwise-in-time a posteriori error control for time-fractional parabolic equations, *Appl. Math. Lett.*, **123** (2022), 107515.

[27] N. Kopteva and X. Meng, Error analysis for a fractional-derivative parabolic problem on quasi-graded meshes using barrier functions, *SIAM J. Numer. Anal.*, **58** (2020), 1217–1238.

[28] D.F. Li, H.L. Liao, W.W. Sun, J.L. Wang, and J.W. Zhang, Analysis of L1-Galerkin FEMs for time-fractional nonlinear parabolic problems, *Commu. Comput. Phys.*, **23** (2018), 86–103.

[29] D.F. Li, C. Wu, and Z. Zhang, Linearized Galerkin FEMs for nonlinear time fractional parabolic problems with non-smooth solutions in time direction, *J. Sci. Comput.*, **80** (2019), 403–419.

[30] X. Li and C. Xu, A space-time spectral method for the time fractional diffusion equation, *SIAM J. Numer. Anal.*, **47** (2009), 2108–2131.

[31] X. Li and C. Xu, Existence and uniqueness of the weak solution of the space-time fractional diffusion equation and a spectral method approximation, *Commun. Comput. Phys.*, **8** (2010), 1016–1051.

[32] Z. Li, Z. Liang, and Y. Yan, High-order numerical methods for solving time fractional partial differential equations, *J. Sci. Comput.*, **71** (2017), 785–803.

[33] H. Liao, D.F. Li, and J.W. Zhang, Sharp error estimate of the nonuniform L1 formula for linear reaction-subdiffusion equations, *SIAM J. Numer. Anal.*, **56** (2018), 1112–1133.

[34] H. Liao, W. Mclean, and J.W. Zhang, A discrete Grönwall inequality with applications to numerical schemes for subdiffusion problems, *SIAM J. Numer. Anal.*, **57** (2019), 218–237.

[35] Y. Lin and C. Xu, Finite difference/spectral approximations for the time-fractional diffusion equation, *J. Comput. Phys.*, **225** (2007), 1533–1552.

[36] A. Lischke, M. Zayernouri, and A. Matzavinos, A Petrov-Galerkin spectral method of linear complexity for fractional multiterm ODEs on the half line, *SIAM J. Sci. Comput.*, **39** (2017), A922–A946.

[37] A. Lozinski, M. Picasso, and V. Prachittham, An anisotropic error estimator for the Crank-Nicolson method: Application to a parabolic problem, *SIAM J. Sci. Comput.*, **31** (2009), 2757–2783.

[38] C. Lubich, Discretized fractional calculus, *SIAM J. Math. Anal.*, **17** (1986), 704–719.

[39] C. Lubich, Convolution quadrature and discretized operational calculus. I, *Numer. Math.*, **52** (1988), 129–145.

[40] C. Lubich, Convolution quadrature revisited, *BIT Numer. Math.*, **44** (2004), 503–514.

[41] C. Lv and C. Xu, Error analysis of a high order method for time-fractional diffusion equations, *SIAM J. Sci. Comput.*, **38** (2016), A2699–A2724.

[42] R. Metzler and J. Klafter, The random walk's guide to anomalous diffusion: A fractional dynamics approach, *Phys. Rep.*, **339** (2000), 1–77.

[43] K. Sakamoto and M. Yamamoto, Initial value/boundary value problems for fractional diffusion-wave equations and applications to some inverse problems, *J. Math. Anal. Appl.*, **382** (2011), 426–447.

[44] S.G. Samko, A.A. Kilbas, and O.I. Marichev, *Fractional Integrals and Derivatives: Theory and Applications*, Gordon and Breach Science Publishers, 1993.

[45] M. Stynes, E. O'Riordan, and J.L. Gracia, Error analysis of a finite difference method on graded meshes for a time-fractional diffusion equation, *SIAM J. Numer. Anal.*, **55** (2017), 1057–1079.

[46] Z.Z. Sun and X. Wu, A fully discrete scheme for a diffusion wave system, *Appl. Numer. Math.*, **56** (2006), 193–209.

[47] R. Verfürth, A posteriori error estimates for finite element discretizations of the heat equation, *Calcolo*, **40** (2003), 195–212.

[48] H. Wang, Y. Chen, Y. Huang, and W. Mao, A posteriori error estimates of the Galerkin spectral methods for space-time fractional diffusion equations, *Adv. Appl. Math. Mech.*, **12** (2020), 87–100.

[49] K. Wang and Z. Zhou, High-order time stepping schemes for semilinear subdiffusion equations, *SIAM J. Numer. Anal.*, **58** (2020), 3226–3250.

[50] W.S. Wang, M.L Mao, and Y. Huang, A posteriori error control and adaptivity for the IMEX BDF2 method for PIDEs with application to options pricing models, *J. Sci. Comput.*, **93** (2022), 5.

[51] W.S. Wang, T. Rao, W.W. Shen, and P. Zhong, A posteriori error analysis for the Crank-Nicolson-Galerkin method for the reaction-diffusion equations with delay, *SIAM J. Sci. Comput.*, **40** (2018), A1095–A1120.

[52] W.S. Wang and L.J. Yi, Delay-dependent elliptic reconstruction and optimal $L^\infty(L^2)$ a posteriori error estimates for fully discrete delay parabolic problems, *Math. Comput.*, **91** (2022), 2609–2643.

[53] W.S. Wang, L.J. Yi, and A.G. Xiao, A posteriori error estimates for fully discrete finite element method for generalized diffusion equation with delay, *J. Sci. Comput.*, **84** (2020), 1–27.

[54] M. Weilbeer, *Efficient Numerical Methods for Fractional Differential Equations and Their Analytical Background*, Dissertation zur Erlangung des Grades eines Doktors der Naturwissenschaften, Technischen Universität Braunschweig, 2005.

[55] Y. Yan, M. Khan, and N.J. Ford, An analysis of the modified L1 scheme for time-fractional partial differential equations with nonsmooth data, *SIAM J. Numer. Anal.*, **56** (2018), 210–227.

[56] Y. Yan, K. Pal, and N.J. Ford, Higher order numerical methods for solving fractional differential equations, *BIT Numer. Math.*, **54** (2014), 555–584.

[57] X. Ye and C. Xu, A posteriori error estimates for the fractional optimal control problems, *J. Inequal. Appl.*, **141** (2015), 1–13.

[58] M. Zayernouri and A. Matzavinos, Fractional Adams-Bashforth/Moulton methods: An application to the fractional Keller-Segel chemotaxis system, *J. Comput. Phys.*, **317** (2016), 1–14.

[59] F. Zeng, C. Li, F. Liu, and I. Turner, The use of finite difference/element approaches for solving the time-fractional subdiffusion equation, *SIAM J. Sci. Comput.*, **35** (2013), A2976–A3000.

[60] F. Zeng, Z. Zhang, and G.E. Karniadakis, Second-order numerical methods for multi-term frac-

tional differential equations: Smooth and non-smooth solutions, *Comput. Methods Appl. Mech. Engrg.*, **327** (2017), 478–502.

[61] H. Zhang, F. Zeng, X. Jiang, and G.E. Karniadakis, Convergence analysis of the time-stepping numerical methods for time-fractional nonlinear subdiffusion equations, *Fract. Calc. Appl. Anal.*, **25** (2022), 453–487.

[62] X. Zhao, X.Z. Hu, W. Cai, and G.E. Karniadakis, Adaptive finite element method for fractional differential equations using hierarchical matrices, *Comput. Methods Appl. Mech. Engrg.*, **325** (2017), 56–76.